

# Bio-inspired Knee Joint Mechanism for a Hydraulic Quadruped Robot

Hamza Khan, Roy Featherstone, Darwin G. Caldwell, Claudio Semini

Department of Advanced Robotics, Istituto Italiano di Tecnologia (IIT)

Email: {hamza.khan, darwin.caldwell, claudio.semini}@iit.it  
roy.featherstone@ieee.org

**Abstract**—Over the last few decades, legged robots are becoming a promising solution for rough terrain navigation, however, existing legged machines often lack versatility to perform a wide range of different gaits. To build a highly dynamic and versatile legged robot, it is essential to have lightweight legs with optimized design and suitable actuators for the desired robot performance and tasks. The design goals are to achieve 1) a wide range of motion for bigger foot workspace which will increase rough terrain walking performance by increasing the number of reachable footholds for each step, 2) optimized joint torque curve since torque output is related to joint angle if linear actuators like pistons are used. In this paper, we focus on the knee joint and propose the adaptation and optimization of the so-called isogram mechanism. It exhibits a changeable *instantaneous center of rotation* (CICR), similar to a human knee joint. We will show how an optimization of design parameters lead to a knee joint design that satisfies the above-mentioned goals. The main contributions of this paper are the kinematic and torque analysis of the isogram mechanism that is actuated by a linear actuator; the optimization of the mechanism’s design parameters; a comparison between the proposed knee joint with the hinge-type knee joint of the quadruped robot HyQ; and experimental results of a proof-of-concept prototype leg featuring the proposed mechanism.

## I. INTRODUCTION

Most of the recent legged robots lack the versatility to perform both precise navigation over rough terrain and the strong, fast motions, that are necessary for dynamic tasks such as jumping and running. Presently very few examples exist besides BigDog [10] by Boston Dynamics and HyQ [14] by IIT. A golden rule for legged robot designers is to reduce the leg’s inertia by moving as much weight close to the torso as possible. At the same time, it is most difficult to find light actuators for the distal joints that meet the required torque, rotational velocity and joint range. These requirements become more challenging when designing a lightweight lower limb for a highly dynamic legged robot.

Even though hydraulic or electric rotary actuators at the knee joint can provide a wide range of motion and flat joint torque curve, their relatively low power-to-mass ratio would make the knee joint heavy and bulky. The quadruped robot StarLETH [6] is a good example for reducing leg inertia while keeping the required knee torque. Its knee actuator is mounted at the hip joint to reduce leg inertia. However, to transmit the motion from the actuator to the joint, StarLETH uses chains that can limit the robustness and performance during highly-dynamic motions. Series elastic actuation (SEA) is used to protect the electric motors and

gearbox from the torque peaks during impacts and to measure and control the joint torque. The elasticity of SEAs however reduces the closed loop control bandwidth.

As shown in one of our most recent works [12], hydraulic actuation is robust against impacts whilst also allowing high-bandwidth control. For this reason presently most mainstream highly dynamic legged robots like HyQ and Boston Dynamics’ machines (BigDog, LS3, Cheetah and ATLAS) use hydraulic actuators instead of electric motors to avoid breakage of reduction gears (an exception is the work presented in [15] where high-torque DC brushless motors with low gear ratio are used to actuate the joints of a highly dynamic quadruped robot). These actuators are installed directly at the joint and therefore no power transmission systems are required. However, these existing dynamic legged robots with linear hydraulic actuators for knee joints lack large range of motion and optimal joint torque curves over the whole range of the linear actuator extension. HyQ and BigDog’s knee joint has a range of motion of around  $120^\circ$ <sup>1</sup>, which makes a successful implementation of tasks like climbing over very rough terrain and self-righting difficult. A few existing legged robots are able to self-right after falling, e.g. NAO [4], Boston Dynamics’ LS3 and ETH’s ALOF [11] thanks to large joint ranges.

The knee joints of most existing legged robots and lower limb exoskeletons are implemented as hinge joints with a fixed axis of rotation. However, a knee joint with a CICR has numerous advantages compared to the classical hinge joint. Possible reasons why current robots do not have knee joints with a CICR are higher complexity and generally bulky implementation. A. Hamon et al. showed in their interesting study [5] that a knee joint with a CICR is better than a knee designed with a revolute joint in terms of energy consumption for legged robots.

In this paper, we proposed an isogram mechanism, which is based on the crossed four-bar linkage [17]. It exhibits a changeable instantaneous center of rotation like a human knee joint. Our objective is not only to enhance the robot performance through the use of a knee joint having CICR but also to map the linear motion of a hydraulic cylinder (high power/weight ratio and ability to cope with impacts) into a revolute joint. And thanks to our new knee joint design,

<sup>1</sup>To the best knowledge of the authors, BigDog’s knee range of motion has not been published. Here it is roughly estimated to be less than  $120^\circ$  based on online videos.

we achieve a  $180^\circ$  joint range and the desired torque profile. Due to our robust low level hydraulic control approach [2], we achieve linear hydraulic actuator active compliance with smooth control.

The paper is structured as follows: first, in Section II we discuss related work and various concepts of knee joint designs in the field of robotics and biomechanics. Then Section III presents the isogram mechanism and the derivation of its kinematics. An optimization for the kinematic parameters of the mechanism is described in Section IV; a comparison has been made between the proposed knee joint with HyQ's hinge joint based knee in Section V. Next, Section VI describes the proof of concept with hardware implementation. Section VII discusses the results obtained and Section VIII concludes the paper.

## II. RELATED WORK

In this section we will first discuss the application of isogram mechanisms and then, we will focus on mechanisms used in the legged robots knee joints.

The mechanisms which utilize a CICR like human joints, are based on a classic representation of the crossed four-bar linkage [17]. But there are also other possible ways of representing it, as Oberg showed in a summary of knee mechanisms with a CICR [7]. Here we are focused on the crossed four-bar linkage for a knee joint, which has also been named in literature as a polycentric four-bar linkage [8]. Most of its uses are in prosthetics [9] and human exoskeletons [8]. The mechanism which is proposed in this paper is called an *Isogram Mechanism*. It uses a cross four-bar linkage driven by a linear hydraulic actuator. In another work, CICR based knee joint for legged robot showed superior performance when compared to a single axis joint in terms of stiffness and mechanical advantage [3]. There are also some examples which exist for quadruped robots which uses additional mechanism for a knee joint like WildCat, LS3 by Boston Dynamics and the Cheetah-cub robot by Sprowitz et al. [16]. But the resulting knee joint suffers from a small range of joint motion which causes a lack of versatility.

## III. ISOGRAM MECHANISM BASED KNEE JOINT

The knee joint proposed in this paper features a mechanism known as *Isogram Mechanism*. In this section we will describe the kinematic analysis of the isogram mechanism based knee joint which mainly consists of two links: a *triangular* and a *cover* link which connect the upper and lower leg segments as shown in Fig. 1.

The triangular link is directly connected to the linear actuator at node 5 which creates a rotation of node 5 about node 1 resulting in a knee joint rotation about the CICR with the help of a cover link. Its other two nodes 1 and 3 are connected with the upper and lower leg segments, respectively. The cover link connects both upper and lower links through node 2 and 4. The black dot in Fig. 1 marked with *ICR* represents the instantaneous center of rotation (ICR), which is the intersection point of the cover and triangular link. Due to a changing center of rotation (polycentric rotation or

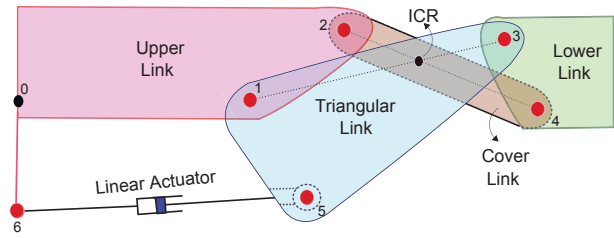


Fig. 1. Schematic representation of the isogram mechanism applied to a legged robot's knee joint. The joint is shown in the fully extended configuration (joint angle  $q = 0^\circ$ ).

CICR) of the proposed knee joint, the definition of the joint angle with respect to cylinder extension has to be derived as explained next.

### A. Knee Joint Angle $q$

The knee joint angle  $q$  is defined as the angle between the longitudinal axis of the upper link and the longitudinal axis of the lower link. It can be expressed as the sum of the angle  $q_1$  (Fig. 2) and  $q_3$  (Fig. 3) as follows:

$$q = 180^\circ - (q_1 + q_3 - \varepsilon_1) \quad (1)$$

where  $\varepsilon_1$  is shown in Fig. 3. Equation (1) results in a knee angle equal to zero when the leg is fully extended (straight) and  $180^\circ$  when it is fully retracted. To obtain a definition of the knee joint angle  $q$  as a function of the cylinder extension  $x_{cyl}$ , we divided the mechanism into two parts.

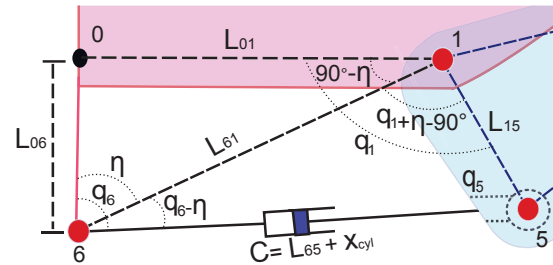


Fig. 2. Isogram mechanism: close-up view of the first half of the mechanism to illustrate angle  $q_1$

First, we have to obtain an expression for  $q_1$  considering only the first half of the mechanism, as shown in Fig. 2. The three side lengths of  $\triangle 0156$   $L_{01}$ ,  $L_{06}$  and  $L_{15}$  are fixed, while length  $C$  is the sum of the cylinder's fully contracted length  $L_{65}$  and the current cylinder extension  $x_{cyl}$ . From the known fixed parameters of  $\triangle 016$  we obtain

$$\eta = \arctan\left(\frac{L_{01}}{L_{06}}\right) \quad (2)$$

and

$$L_{61} = \sqrt{L_{01}^2 + L_{06}^2} \quad (3)$$

With the law of cosines applied to  $\triangle 156$  we obtain

$$q_1 = 90^\circ - \eta + \arccos\left(\frac{(L_{61}^2 + L_{15}^2 - C^2)}{2L_{61}L_{15}}\right) \quad (4)$$

Let us now consider Fig. 3 to calculate  $q_3$ . It is defined as

$$q_3 = \beta - \varepsilon_3 - \phi + \lambda \quad (5)$$

where  $\lambda$  is defined as  $\lambda = \arccos(\frac{X_{34}}{L_{34}})$  and we already know the dimensions of the triangular link, which are fixed lengths ( $L_{13}$ ,  $L_{15}$  and  $L_{35}$ ). Its angles ( $\varepsilon_1$ ,  $\varepsilon_2$  and  $\varepsilon_3$ ) can be expressed using the law of cosines. Using the law of cosines

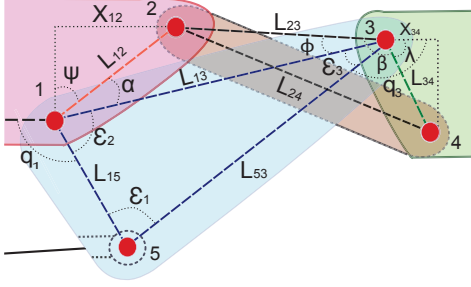


Fig. 3. Isogram mechanism: close-up view of the second half of the mechanism to illustrate angle  $q_3$

at  $\triangle 123$ , the virtual length  $L_{23}$  can be expressed as

$$L_{23} = \sqrt{L_{13}^2 + L_{12}^2 - 2L_{13}L_{12} \cos \alpha} \quad (6)$$

where  $\alpha$  is defined as

$$\alpha = 270^\circ - q_1 - \varepsilon_2 - \psi \quad (7)$$

and  $\psi$  is given  $\psi = \arcsin(\frac{L_{12}}{X_{12}})$ . Once we calculated the virtual length  $L_{23}$ , we can express  $\phi$  as follows

$$\phi = \arccos\left(\frac{L_{23}^2 + L_{13}^2 - L_{12}^2}{2L_{23}L_{13}}\right) \quad (8)$$

Similarly, we obtain

$$\beta = \arccos\left(\frac{L_{23}^2 + L_{34}^2 - L_{24}^2}{2L_{23}L_{34}}\right) \quad (9)$$

Using (8) and (9), we can rewrite (5) as follows

$$q_3 = \lambda - \varepsilon_3 + \arccos\left(\frac{L_{23}^2 + L_{34}^2 - L_{24}^2}{2L_{23}L_{34}}\right) - \arccos\left(\frac{L_{23}^2 + L_{13}^2 - L_{12}^2}{2L_{23}L_{13}}\right) \quad (10)$$

At last we obtain the analytical solution of the knee joint angle  $q$  in relation to piston position  $x_{cyl}$ :

$$q = 90^\circ + \varepsilon_1 + \eta - \lambda + \varepsilon_3 - \arccos\left(\frac{L_{61}^2 + L_{15}^2 - (L_{65} + x_{cyl})^2}{2L_{61}L_{15}}\right) - \arccos\left(\frac{L_{23}^2 + L_{34}^2 - L_{24}^2}{2L_{23}L_{34}}\right) + \arccos\left(\frac{L_{23}^2 + L_{13}^2 - L_{12}^2}{2L_{23}L_{13}}\right) \quad (11)$$

## B. Knee Joint Torque $\tau$

The knee joint torque  $\tau$  depends on the current cylinder extension  $x_{cyl}$  and cylinder force  $F$ . As the knee joint angle  $q$  is a function of the cylinder extension  $x_{cyl}$ ,  $q = f(x_{cyl})$ , the knee joint torque  $\tau$  be written as

$$\tau = \frac{dx_{cyl}}{dq} F \quad (12)$$

where

$$\frac{dx_{cyl}}{dq} = \frac{df(x_{cyl})^{-1}}{dx_{cyl}} \quad (13)$$

## IV. PARAMETRIC OPTIMIZATION PROBLEM

The mechanism presented in the previous section has a set of 11 design parameters (namely the lengths  $L_{24}$ ,  $L_{34}$ ,  $L_{13}$ ,  $L_{35}$ ,  $L_{15}$ ,  $L_{01}$ ,  $L_{12}$ ,  $x_{12}$ ,  $x_{34}$ ,  $L_{06}$ ,  $L_{65}$ ) that have to be determined by the designer. This section explains how we optimized this parameter set to obtain a knee joint behavior that meets our requirements.

Such requirements are specified in terms of torque output profile and joint range. According to our group's experience in the development and control of versatile legged robots such as HyQ [1], [13], [14], the following joint range and torque profile are desirable for the knee joint design of agile and versatile quadruped robots (see Section V for more details on this choice): A smoothly distributed torque profile is desired that provides high torque in a retracted joint configuration (i.e. flexed leg) and high velocity (but lower torque) when approaching the fully extended configuration. Furthermore, a large knee joint range  $q$  from 0 to  $180^\circ$  is desired.

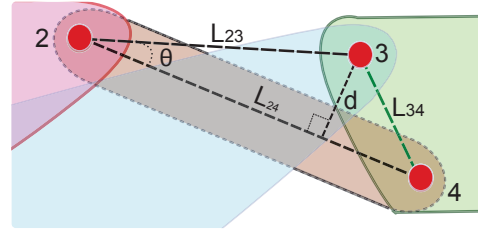


Fig. 4. Isogram mechanism: close-up view of the cover link.

## A. The Objective Function

This section defines the objective function and gets an optimized set of design variables  $P = [L_{24}, L_{34}, L_{13}, L_{35}, L_{15}, L_{01}, L_{12}, x_{12}, x_{34}, L_{06}, L_{65}]$ . The objective function consists of two component: the first one penalizes any design in which  $d$  gets too close to zero.  $d$  is the shortest distance between  $L_{24}$  and node 3 as shown in Fig. 4 and expressed as

$$d = L_{23} \sin(\theta) \quad (14)$$

where  $\theta$  is defined as

$$\theta = \arccos\left(\frac{L_{23}^2 + L_{24}^2 - L_{34}^2}{2L_{23}L_{24}}\right) \quad (15)$$

The second component rewards a smooth, gradual variation from cylinder extension to knee angle and favours a bigger Jacobian (13) at  $q = 0^\circ$  and a smaller one at  $q = 180^\circ$ . This latter is achieved with a quadratic function as mentioned below. The objective function is defined as

$$Y(P) = W_1 * \frac{1}{\min(d)} + W_2 * \sum_{x_{cyl}=1}^{66} (q - q_l)^2 \quad (16)$$

We have an ideal  $q_l$  in mind, that is part of the optimization, but at the same time we need to keep the overall knee dimensions small. Therefore, we introduced the minimization of  $d$  in the objective function. Where  $\min(d)$  is the minimum value of variable  $d$  over the whole range of cylinder extension ( $x_{cyl} = 0$  to 67 mm).  $q_l$  linearize knee joint angle is defined as a quadratic function  $q_l = a_2 * x_{cyl}^2 + a_1 * x_{cyl} + a_0$  which has to satisfy the following conditions:

- $x_{cyl} = 0$  when  $q = 180^\circ$  and  $x_{cyl} = 67mm$  when  $q = 0^\circ$
- its slope at  $x_{cyl} = 67mm$  is equal to twice the slope at  $x_{cyl} = 0mm$

which leads to  $a_0 = 180$ ,  $a_1 = -1.79$  and  $a_2 = -0.0134$  after solving the quadratic function.

### B. The constraints

The equality constraints are defined on the basis of the following conditions:

- $Y(P) = K$  if a close loop kinematics solution does not exist
- $q = 180^\circ$  if  $x_{cyl} = 0mm$
- $q = 0^\circ$  if  $x_{cyl} = 67mm$

To obtain realistic design variables, we constrained the objective function so that if a close loop kinematics solution does not exist,  $Y(P) = K$ , where  $K$  is a large value (set to  $1e8$  here). This condition penalizes the sets of parameters  $P$  for which a geometric solution does not exist. The other two conditions make sure that the cylinder's stroke length spans the entire range of desired knee joint angles.

### C. Optimization result

The main goal of this optimization is to get a desired torque profile that is large for a flexed leg configuration and small when extended. Figure 5 shows the optimized knee joint torque profile (solid blue line) with respect to knee angle. Its highest torque output lies where the knee is almost completely retracted ( $q = 150^\circ$  to  $180^\circ$ ). The red dashed line in this figure shows the result of an initial guess for the values of the parameter set  $P$ . The Matlab function *fmincon* is used to minimize the cost function (16). We tried different initial conditions, which satisfy the constraints defined in section IV-B. Table I shows the set of design variables.

The design of the knee joint mechanism is based on optimized results. For the optimization, we fixed two design variables ( $L_{65}, L_{06}$ ). The length  $L_{65}$  is the eye-to-eye distance of the fully retracted cylinder and given by the cylinder design, load cell and rod end length. The variable  $L_{06}$  is the distance between reference node 0 to cylinder mounting node

TABLE I  
OPTIMIZED DESIGN VARIABLES

Design variables	Initial guess (mm)	Optimized values (mm)
$L_{24}$	67	75
$L_{34}$	32	28
$L_{13}$	69	75.5
$L_{35}$	75	70
$L_{15}$	45	38.7
$L_{01}$	211	205
$L_{12}$	36	35
$x_{12}$	12	18
$x_{34}$	15	22
$L_{06}$	fixed	59
$L_{65}$	fixed	180.5

6 as shown in Fig. 1. We fixed  $L_{06}$  to keep space for leg electronics and hydraulic manifold which has to fit inside the upper link. The initial guess for mechanism link lengths were found by trail and error. Reasonable upper and lower bound of each design variable were defined. Random initial guesses are chosen from these ranges to avoid local minimum. The results are shown in Fig. 5 to show the effectiveness of numerical optimization.

Figure 5 (right) shows the knee joint angle  $q$  with change in cylinder extension  $x_{cyl}$ . The torque profiles shown in Fig.

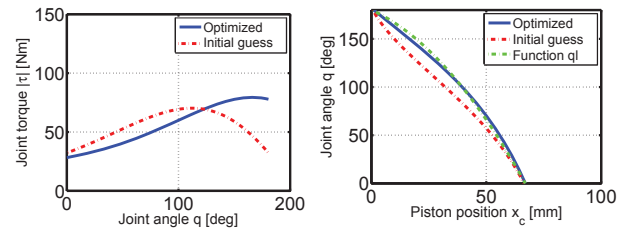


Fig. 5. (left) Isogram knee joint torque profile with respect to knee angle; (right) knee joint angle vs. piston position; where the blue solid line indicates the optimized results; the red dot dashed line is the result of an initial guess based on trail and error method; the green dashed line shows the quadratic function  $q_l$  with respect to piston position.

5 are based on a maximum actuator force  $F = 2653N$  that results from an extending cylinder at a pressure of  $20MPa$ . (The selected cylinder has a bore diameter of 13mm and a rod diameter of 6mm). The weights for the objective function are selected in a heuristic way and a priori knowledge is used to determine a best set of weights  $W_1 = 0.3$  and  $W_2 = 0.6$ . The selection of the weights is further discussed in Section VII.

### V. HYQ'S KNEE VS OPTIMIZED ISOGRAM KNEE

HyQ [14] is a fully torque-controlled Hydraulically actuated Quadruped robot developed at the Department of Advanced Robotics of IIT Genova, shown in Fig. 6 (left). HyQ is designed to move over rough terrain and perform highly dynamic tasks such as jumping and running with different gaits (up to 2m/s). To achieve the required high

joint speeds and torques, hydraulic actuators are powering the robot's 12 active joints. Its torso and legs are constructed from an aerospace-grade aluminum alloy. HyQ's knee possesses a revolute joint shown in Fig. 6 (right) that uses a linear hydraulic actuator directly mounted between the upper and lower leg. The distance from the cylinder attachment point to the knee joint is 45mm, which results in a maximum joint torque of 145Nm at 16MPa. The knee range is  $120^\circ (q = 20^\circ \text{ to } 140^\circ)$ .

*Why do we need an isogram knee joint?*

The motivation of this work is strongly influenced by the experience of our group with the quadruped robot HyQ. Even though the robot demonstrated many different motions and gaits, the robot has certain limitations that make it difficult or impossible to perform certain motions. For example during one of our recent experiments where HyQ walked over obstacles with planned footholds in a 3D map [18]: When stepping onto a pallet, stairs or over obstacles, the limited knee joint range made it difficult to retract the leg enough to avoid collisions.

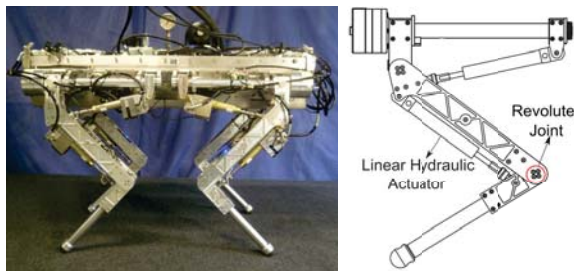


Fig. 6. HyQ: Hydraulic Quadruped robot. (left) picture of the robot. (right) drawing of HyQ's Leg with a red circle highlighting its revolute knee joint.

Here we considered a squat jump as example motion to demonstrate the importance of suitable knee joint torque profile for a highly dynamic robot. We used the experimental data of HyQ performing a squat jump with 0.2m jump height [13]. A squat jump is composed of several phases: first, a vertical *acceleration phase* from a squatting posture until lift-off; then, a parabolic *flight phase* with the legs moving to a suitable landing posture. The three subplots of Fig. 7 show the data of the experiment (red solid line) and of the simulation (black dashed line with 0.2m jump height where blue dashed line shows simulation results for 0.3m jump height) for the knee joint angle (top), knee joint torque (middle) and vertical ground reaction force (bottom). The acceleration phase of the experiment starts at 0.1s and lasts till 0.4s when the torques go to zero. The robot touches down again at 0.78s. The simulation calculates values only during the acceleration phase.

The comparison shown in Fig. 8 illustrates the advantages of the new knee mechanism over the existing HyQ knee. Here the effective lever arm is obtained by scaling the joint torque profile by the maximum output force of the cylinder. The red dashed line shown in Fig. 8 represents HyQ's knee effective lever arm with respect to joint angle and the solid

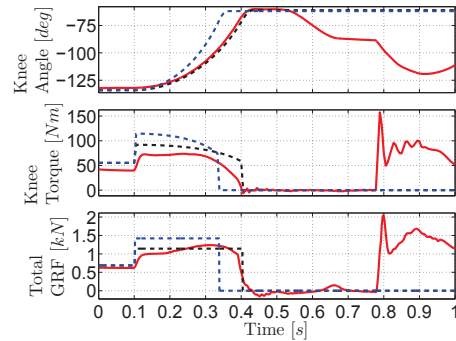


Fig. 7. Plot of experimental data of HyQ (red solid), simulated data (black dashed) for a squat jump motion of 0.2m jump height, where simulated data (blue dashed) is at 0.3m jump height. Top: knee joint angle; middle: knee torque; bottom: total ground reaction force. (Figure modified from [13])

blue line indicates the scaled isogram knee joint angle vs. effective lever arm. The maximum force of the cylinder that drives HyQ's knee is 3217N (16 mm bore cylinder at 16MPa). p3 in Fig. 6 indicates HyQ's knee peak joint torque at  $80^\circ$  knee angle which is 145Nm ( $3217N * 0.045m$ ).

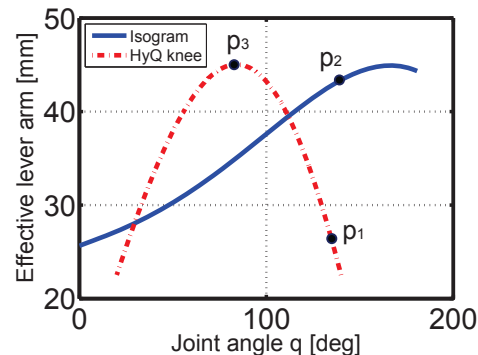


Fig. 8. Shows the comparison of the effective lever arm between HyQ's knee joint and scaled optimized isogram knee joint during knee extension

It is shown in Fig. 7 that HyQ during a squat jump requires the maximum torque in almost retracted knee configuration. It is marked as p1 in Fig. 8 at  $135^\circ$  joint angle, the effective lever arm is 25.5 mm which gives 82Nm ( $3217N * 0.0255m$ ) joint torque. HyQ can safely perform squat jump of 0.2m jump height with 70 kg body weight within its joint torque limit. But simulation data (blue dashed) shown in Fig. 7) showed that HyQ knee would need 117Nm at  $135^\circ$  knee angle to perform 0.3m high jump. Since its peak torque (at p3) lies in the center of HyQ's  $120^\circ$  range of motion which tails out very quickly when the knee is almost retracted, HyQ is not capable to utilize its maximum torque to preform 0.3m high jump. But in case of isogram knee joint at  $135^\circ$  joint angle, it provides 137Nm ( $3217N * 0.0424m$ , scaled value) which is indicated by p2 shown in Fig. 8. The solid blue curve shows optimized torque profile of isogram knee joint where its torque distribution is close to the desired shape. While HyQ's knee joint range of motion is restricted to  $120^\circ (q = 20^\circ \text{ to } 140^\circ)$ , the isogram knee provides  $180^\circ (q = 0^\circ \text{ to } 180^\circ)$ . From the shown torque

profiles, it can be concluded that the optimized isogram knee mechanism exhibits a larger range of motion and the desired torque profile.

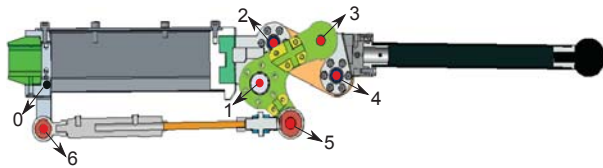


Fig. 9. CAD model, Cross sectional view of the knee joint based on optimization results (similar kinematic representation to Figure 1).

## VI. PROOF OF CONCEPT WITH HARDWARE IMPLEMENTATION

As a proof of concept we built and tested an early design of the knee joint mechanisms as shown in Fig. 10. The implemented design is according to optimization results. The upper link is built with a folded 1.5mm aluminium sheet and the lower link with a square-section carbon fiber rod. The knee mechanism is constructed with machined aluminium parts and ball bearings with tight tolerances to avoid backlash in the mechanism.



Fig. 10. Hardware implementation. *Left*: Side view of the *isogram mechanism* based knee joint; *Right*: close up view of load cell and encoders.

Due to the CICR, it is not possible to install position sensors that directly measure the joint angle. Therefore, we installed absolute and relative (high-resolution) encoders at node 1 (see Fig. 1) to measure  $q_1$  that can then be mapped into a joint angle using (1), (10) and (11). To measure the joint torque we installed a load cell in series with the cylinder rod that measures the cylinder force that can then be mapped into a torque using (12). A miniature servo valve is used to control the cylinder force and joint angle.

### Experimental results

To check the stability of hardware, we performed *push ups* motion. The experimental setup is shown in Fig 11, where the upper leg is attached to a revolute hip joint. A Push ups task is preformed by moving the foot in a vertical trajectory below the hip joint at 0.5Hz with 12kg payload. Results are shown in Fig. 12. Figure 13 shows a picture sequence of an experimental motion through the whole joint range of motion.

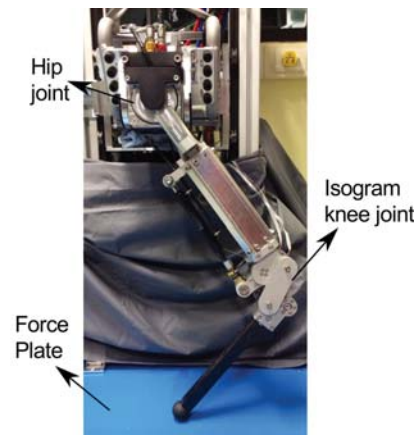


Fig. 11. Experimental setup for performing push ups. The upper leg is attached to a revolute hip joint. A Kistler force plate is used to measure the ground reaction forces (GRF). The whole setup is connected a slider which allows it to move freely up and down (vertically).

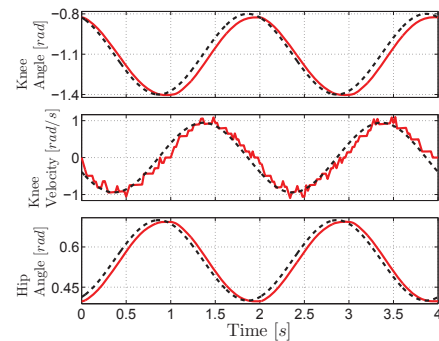


Fig. 12. Plot of experimental measured data of isogram knee (red solid), reference data (black dashed) for push ups at 0.5Hz (with 12Kg payload). *Top*: knee joint angle; *middle*: knee velocity; *bottom*: Hip joint angle.

## VII. DISCUSSION

We demonstrated that despite its higher complexity, the isogram mechanism is superior to the traditional design, because its many kinematic parameters can be fine-tuned to achieve an optimal torque profile. Such profiles should preferably lead to a robotic leg that is strong in a flexed configuration and fast when almost extended. We demonstrated how smooth and optimized torque profiles can be obtained by parameter optimization.

The weights  $W_1$  and  $W_2$  are currently selected in a heuristic way. A more detailed study of the influence of these weights is required. Furthermore, we noticed that if we penalize  $d$  in the objective function we might end up with solutions that favor larger overall sizes of the mechanism. Since we aim for compact and lightweight designs, instead of penalizing small  $d$ , an objective function that keeps the angle  $\beta$  away from  $180^\circ$  might be more suitable since it does not lead to larger designs.

## VIII. CONCLUSION AND FUTURE WORK

This paper compared two different mechanisms for legged robots knee joints that are driven by linear actuators such

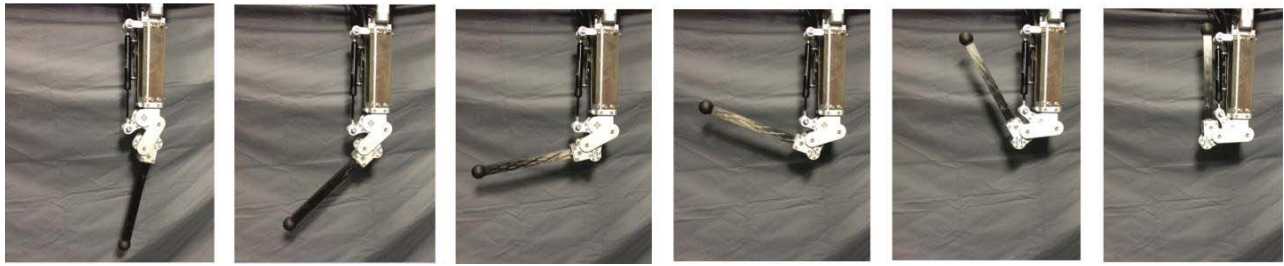


Fig. 13. Picture sequence of the prototype leg during an experiment that moves the knee joint from extended to completely retracted position.

as hydraulic cylinders. The first mechanism is the traditional approach where the cylinder is directly connected between the upper and lower leg segment via a configuration-dependent lever arm. In the second design, the leg segments and cylinder are connected through the so-called isogram mechanism. An early prototype leg featuring the presented isogram mechanism has been experimentally tested. The leg will be part of a small, light-weight and versatile hydraulic quadruped called *MiniHyQ*. *MiniHyQ* will be a torque-controlled robot that is able to walk, move over rough terrain, jump and run. More tests will be done in the future on *MiniHyQ*'s leg prototype. In the future, further improvement will be done to make this design more compact and optimal for the final version of *MiniHyQ* knee. Further studies will be performed to analyze the effects of a CICR knee joint on the performance of quadruped robot locomotion.

#### APPENDIX – VIDEO CONTENTS

At the given video link, the summary of this work is shown which includes experiments performed on the proposed knee joint.

<http://youtu.be/81pZQjzFULk>

#### ACKNOWLEDGMENTS

The authors would like to thank also the colleagues that collaborated for the success of this project: Victor Barasuol, Michele Focchi, Jake Goldsmith, Marco Frigerio, Bilal Ur Rehman, Ioannis Havoutis and our team of technicians. This research has been funded by the Fondazione Istituto Italiano di Tecnologia.

#### REFERENCES

- [1] V. Barasuol, J. Buchli, C. Semini, M. Frigerio, E. R. De Pieri, and D. G. Caldwell. A reactive controller framework for quadrupedal locomotion on challenging terrain. In *IEEE International Conference on Robotics and Automation (ICRA)*, 2013.
- [2] T. Boaventura, G.A. Medrano-Cerda, C. Semini, J. Buchli, and D. G. Caldwell. Stability and performance of the compliance controller of the quadruped robot hyq. In *IEEE/RSJ International Conference on Intelligent Robots and Systems (IROS)*, 2013.
- [3] A. C. Etoundi, R. Vaidyanathan, and S. C. Burgess. *A bio-inspired condylar hinge joint for mobile robots*, pages 4042–4047. Institute of Electrical and Electronics Engineers, Sep 2011.
- [4] D. Gouaillier, V. Hugel, P. Blazevic, C. Kilner, J. Monceaux, P. Lafourcade, B. Marnier, J. Serre, and B. Maisonnier. Mechatronic design of nao humanoid. In *2009 IEEE International Conference on Robotics and Automation*, pages 769–774, May 2009.
- [5] A. Hamon and Y. Aoustin. Cross four-bar linkage for the knees of a planar bipedal robot. In *2010 10th IEEE-RAS International Conference on Humanoid Robots*, pages 379–384, Dec 2010.
- [6] M. Hutter, C. D. Remy, M. A. Hoepflinger, and R. Siegwart. Efficient and versatile locomotion with highly compliant legs. *IEEE/ASME Transactions on Mechatronics*, 18(2):449–458, Apr 2013.
- [7] K. Oberg. Knee mechanisms for through-knee prostheses. In *Prosthetics and orthotics international*, 1983.
- [8] S. Pfeifer, R. Riener, and H. Vallery. An actuated transfemoral prosthesis with optimized polycentric knee joint. In *2012 4th IEEE RAS & EMBS International Conference on Biomedical Robotics and Biomechanics (BioRob)*, pages 1807–1812, Jun 2012.
- [9] CW. Radcliffe. Four-bar linkage prosthetic knee mechanisms: Kinematics, alignment and prescription criteria. In *Prosthetics and orthotics international*, 1994.
- [10] M. Raibert, K. Blankespoor, G. Nelson, R. Playter, and the Big-Dog Team. Bigdog, the rough-terrain quadruped robot. In *IFAC*, 2008.
- [11] C. David Remy, Oliver Baur, Martin Latta, Andi Lauber, Marco Hutter, Mark A. Hoepflinger, Cdric Pradalier, and Roland Siegwart. Walking and crawling with alof: a robot for autonomous locomotion on four legs. *Industrial Robot: An International Journal*, 38(3):264 – 268, 2011.
- [12] C. Semini, V. Barasuol, T. Boaventura, M. Frigerio, and J. Buchli. Is active impedance the key to a breakthrough for legged robots? In *International Symposium of Robotics Research (ISRR)*, 2013.
- [13] C. Semini, H. Khan, M. Frigerio, T. Boaventura, M. Focchi, J. Buchli, and D. G. Caldwell. Design and scaling of versatile quadruped robots. In *CLAWAR Conference*, 2012.
- [14] C. Semini, N G. Tsagarakis, E. Guglielmino, M. Focchi, F. Cannella, and D G. Caldwell. Design of HyQ - a hydraulically and electrically actuated quadruped robot. *IMEchE Part I: J. of Systems and Control Engineering*, 225(6):831–849, 2011.
- [15] S. Seok, A. Wang, Meng Y. C., D. Otten, J. Lang, and S. Kim. Design principles for highly efficient quadrupeds and implementation on the MIT cheetah robot. *2013 IEEE International Conference on Robotics and Automation*, May 2013.
- [16] A. Sprowitz, A. Tuleu, M. Vespignani, M. Ajallooeian, E. Badri, and A. J. Ijspeert. Towards dynamic trot gait locomotion: Design, control, and experiments with cheetah-cub, a compliant quadruped robot. *The International Journal of Robotics Research*, 32(8):932–950, Jul 2013.
- [17] A. G. Steven, S. C. Dudley, and E. U. Jack. The influence of four-bar linkage knees on prosthetic swing-phase floor clearance. *Journal of Prosthetics and Orthotics*, 8(2):34–40, 1996.
- [18] A. Winkler, I. Havoutis, S. Bazeille, J. Ortiz, M. Focchi, R. Dillmann, D. G. Caldwell, and C. Semini. Path planning with force-based foothold adaptation and virtual model control for torque controlled quadruped robots. In *IEEE International Conference in Robotics and Automation*, 2014.